



# Exhaustive *in vitro* evaluation of the 9-drug cocktail CUSP9 for treatment of glioblastoma

Efthymia Chantzi<sup>a</sup>, Ulf Hammerling<sup>b</sup>, Mats G. Gustafsson<sup>b,\*</sup>

<sup>a</sup> Department of Medical Sciences, Cancer Pharmacology and Computational Medicine, Uppsala University, Sweden

<sup>b</sup> Department of Civil & Industrial Engineering, Industrial Analytics, Uppsala University, Sweden

## ARTICLE INFO

### Keywords:

Glioblastoma multiforme  
CUSP9  
Personalized medicine  
Deep learning  
Live-cell imaging  
COMBImageDL

## ABSTRACT

The CUSP9 protocol is a polypharmaceutical strategy aiming at addressing the complexity of glioblastoma by targeting multiple pathways. Although the rationale for this 9-drug cocktail is well-supported by theoretical and *in vitro* data, its effectiveness compared to its 511 possible subsets has not been comprehensively evaluated. Such an analysis could reveal if fewer drugs could achieve similar or better outcomes.

We conducted an exhaustive *in vitro* evaluation of the CUSP9 protocol using COMBImageDL, our specialized framework for testing higher-order drug combinations. This study assessed all 511 subsets of the CUSP9v3 protocol, in combination with temozolomide, on two clonal cultures of glioma-initiating cells derived from patient samples. The drugs were used at fixed, clinically relevant concentrations, and the experiment was performed in quadruplicate with endpoint cell viability and live-cell imaging readouts. Our results showed that several lower-order drug combinations produced effects equivalent to the full CUSP9 cocktail, indicating potential for simplified regimens in personalized therapy. Further validation through *in vivo* and precision medicine testing is required.

Notably, a subset of four drugs (auranofin, disulfiram, itraconazole, sertraline) was particularly effective, reducing cell growth, altering cell morphology, increasing apoptotic-like cells within 4–28 h, and significantly decreasing cell viability after 68 h compared to untreated cells.

This study underscores the importance and feasibility of comprehensive *in vitro* evaluations of complex drug combinations on patient-derived tumor cells, serving as a critical step toward (pre-)clinical development.

## 1. Introduction

Glioblastoma multiforme (GBM) is a highly aggressive brain tumor, characterized by its notorious resistance to conventional pharmacotherapy and a grim prognosis for patients [1]. The disease is further complicated by the complex inter- and intra-tumor heterogeneity, widely recognized as a primary driver of therapy resistance and disease progression [2–4].

In response to this clinical challenge, the adoption of polypharmaceutical approaches involving multi-drug cocktails, often consisting of three or more agents, has gained increasing interest and traction. A prominent example is the CUSP9v3 protocol [4–8]. Comprising nine repurposed (non-oncological) drugs — aprepitant (Apr), auranofin (Aur), captopril (Cap), celecoxib (Cel), disulfiram (Dis), itraconazole (Itr), minocycline (Min), ritonavir (Rit) and sertraline (Ser). CUSP9v3 is thoughtfully designed to target known growth and survival pathways implicated in GBM. The ultimate objective is to synergize with temozolomide (TMZ), the standard-of-care drug, making it more effective [5,

6]. It is worth noting that the protocol has undergone a phase Ib/IIa clinical trial (NCT02770378) when used as an adjunct to TMZ, demonstrating a tolerable safety profile, especially with the necessary dose adjustment of aprepitant due to interactions with itraconazole [8].

Many studies have highlighted the potential of higher-order drug combinations and single multi-targeting drugs for treating complex diseases, including cancer [9–12]. Notably, Cao et al. [13] demonstrated that CUSP9, combined with tumor-treating electrical fields, induces metabolic reprogramming and synergistic anti-glioblastoma effects *in vitro*. Furthermore, our use of fixed concentrations in this *in vitro* study aligns with the growing clinical interest in fixed-dose combination therapies, such as those used to prevent atherosclerotic cardiovascular disease [14].

Despite the promising theoretical framework that paved the way for the CUSP9 regimen, its clinical implementation preceded comprehensive *in vitro* and subsequent *in vivo* evaluations, which could strengthen its therapeutic potential. The first *in vitro* experimental results on the

\* Corresponding author.

E-mail addresses: [efthymia.chantzi@medsci.uu.se](mailto:efthymia.chantzi@medsci.uu.se) (E. Chantzi), [mats.gustafsson@angstrom.uu.se](mailto:mats.gustafsson@angstrom.uu.se) (M.G. Gustafsson).

combined effect of CUSP9 and TMZ on patient-derived GBM stem cells were published in 2019 by Skaga et al. [15]. Two years later, when the clinical trial assessing the safety of CUSP9v3 was near completion, another study was published, offering additional *in vitro* insights and clinical compassionate use experiences with the CUSP9v3 approach [4]. In both cases, the efficacy of TMZ was found to be substantially enhanced by the CUSP9 cocktail, thereby adding valuable pre-clinical evidence for this polypharmacotherapeutic approach.

One of the important questions that remains unresolved is whether the inclusion of all nine drugs is necessary to achieve maximal therapeutic effect [4]. Addressing this question is a complex endeavor, as it requires a comprehensive evaluation of the combined effects of these drugs in both *in vitro* and *in vivo* settings to ensure robust clinical predictability. However, when it comes to large-scale drug combination screening, conducting extensive *in vivo* testing becomes increasingly impractical, unrealistic, and ethically challenging [16]. Therefore, a thorough *in vitro* assessment of the CUSP9v3 cocktail presents a promising initial step in gathering preliminary evidence regarding the potential of achieving an equivalent or even superior effect using subsets of the nine drugs. Such data could provide valuable support for the selection of individualized GBM therapies, maximizing effectiveness and minimizing adverse effects. For instance, the scope of pre-clinical *in vitro* sensitivity testing of patient-derived GBM cells, used to guide the selection of clinical pharmacotherapy regimens could be expanded to encompass not only the complete CUSP9 cocktail but also its most potent lower-order combinations [17,18]. This analytical framework could pave the way for tailored CUSP9 pharmacotherapy, accommodating the observed heterogeneous drug response patterns highlighted in previous studies [4,15].

To embark on this uncharted journey, we leveraged COMBImageDL, an enhanced deep learning (DL) [19] iteration of our previously introduced framework, COMBImage2 [20]. Our objective was to carefully plan, execute, and analyze an exhaustive *in vitro* experiment involving the CUSP9v3 protocol. Through the capabilities of COMBImageDL, we were able to conduct a comprehensive assessment of all 511 conceivable subsets of this nine-drug cocktail when used in conjunction with TMZ. To execute this experiment, we procured two patient-derived GBM stem-like cell lines of proneural type from the Human Glioblastoma Cell Culture (HGCC) resource [21]. These cell lines were subjected to precise, clinically feasible drug concentrations, with their temporal responses monitored through label-free live-cell imaging. Subsequently, an endpoint cell viability assay was conducted after 68 hours of treatment. To ensure robustness and comprehensively account for experimental variability, the experiment was performed in quadruplicate, spanning a total of sixteen 384-well plates. Notably, this type of detailed information, despite its immense value, is often underutilized due to lack of specialized tools like COMBImageDL.

Our exhaustive *in vitro* assessment of the CUSP9v3 protocol yielded several intriguing findings, further illuminating its potential. Particularly, it reaffirmed the notably enhanced efficacy of the complete nine-drug cocktail when combined with TMZ, consistent with previous findings [4,15]. This, in turn, contributes additional *in vitro* experimental support to the existing body of evidence. However, the standout discovery in our study was the emergence of a distinctive set of drug response patterns involving only three to six drugs as additions to TMZ. Remarkably, these responses matched, and in certain instances exceeded, the efficacy of the entire CUSP9v3 cocktail across both patient derived GBM cell lines employed in our study.

While it is worth noting that the specific lower-order drug combinations displaying such potency varied between the two cell lines, a common denominator emerged in the form of a five-drug combination; comprising Aur, Dis, Itr, Ser and TMZ. The effects induced by this particular combination were striking and included reduced cell growth, notable changes in cell culture morphology, an increased number of apoptotic-like cell counts as early as 4-28 h into treatment, and significantly decreased cell viability compared to untreated cells after 68 hours.

In summary, the main motivations and gaps in the literature behind this work are:

- i. CUSP9 and other suggested higher-order drug combinations are not always subject to systematic *in vitro* evaluations before being tested in animal models and/or clinical trials.
- ii. For each individual patient, most likely a subset of a broad cocktail like CUSP9 will be sufficient, and perhaps even more potent, with less adverse side effects. However, to which extent this is true is largely unknown. Systematic experimental procedures are needed to guide personalized combination therapy selection in the clinic.
- iii. The potential of higher-order combinations as cancer treatment candidates can easily be motivated by the fact that cancer is a complex disease, where multiple distorted biochemical processes are working synergistically together. However, very few systematic studies of such combinations have been reported, so the potential is still largely unexplored.
- iv. There is a general lack of experimental–computational frameworks that enable systematic test tube analyses of higher-order drug cocktails within and beyond cancer pharmacology.

In the light of these motivations and gaps, the key contributions of this work could be summarized below:

- i. A first experimental–computational framework (COMBImageDL) of its kind, which enables systematic test tube analysis of higher-order drug cocktails based on deep learning and tailor made exploratory data analytics.
- ii. A first systematic and comprehensive phenotypic based *in vitro* evaluation and comparison of all 511 drug combination subsets of the 9-drug cocktail CUSP9 for treatment of glioblastoma. The resulting and publicly available dataset is unique as it was performed in quadruplicate, spanning a total of sixteen 384-well plates.
- iii. Identification of lower-order drug cocktails having equal or greater *in vitro* effects compared to the original 9-drug cocktail, for example the 4-drug cocktail comprising auranofin, disulfiram, itraconazole and sertraline.
- iv. A confirmation that higher-order drug combinations are very promising for eradicating complex diseases like cancer and that there is great potential in making them individualized (or at least tumor type specific) based on systematic test tube analyses.
- v. A demonstration that it is feasible and important to perform, analyze, and interpret comprehensive *in vitro* evaluations of higher-order drug cocktails on different disease models and patient derived tumor cells, as a precursor to subsequent (pre-)clinical assessment.

## 2. Material and methods

### 2.1. Cell cultures

The patient derived GBM cell lines *U3082* and *U3118* [21], were cultured in neural stem cell media (1:1 mix of DMEM-F12 GlutaMAX medium and Neurobasal medium (Life Technologies, GIBCO-Invitrogen) containing 1% penicillin G/streptomycin sulfate (Sigma-Aldrich, St. Louis, MO), supplemented with B-27 without vitamin A (1:50; Invitrogen), N2 supplement (1:100; Invitrogen), 10 ng/mL EGF and 10 ng/mL FGF-2 (PeproTech, Rocky Hill, NJ). Cells were seeded in poly-L-ornithine (P4957, Sigma-Aldrich) and laminin (L2020, Sigma-Aldrich) coated 384-well plates (164688, Thermo Fisher Scientific) at a density of 1000 cells/well using a BioMek 4000 (Beckman Coulter). All cells were seeded 24 h prior to treatment with compounds.

## 2.2. Chemical compounds

The CUSP9v3 protocol [4] was employed (Table 1). For all drugs including TMZ, a fixed concentration was determined by an initial dose response experiment on both GBM cell lines and reported blood-plasma levels [22–25]. The goal was to choose for each drug a concentration that induces modest effect *in vitro* (i.e., higher than 80% cell survival), while being within levels achievable *in vivo*.

## 2.3. Assay for determination of survival index

Cell survival was determined by means of the Fluorometric Cytotoxicity Assay (FMCA) [26]. For a particular drug combination concentration vector  $\mathbf{c}_n$  consisting of  $n$  drugs, the cell survival or otherwise survival index, denoted here as  $S$ , is determined as:

$$S(c_{1n}, c_{2n}, \dots, c_{dn}) = S(\mathbf{c}_n) = \frac{f(\mathbf{c}_n) - \bar{f}_{blank}}{\bar{f}_{control} - \bar{f}_{blank}} \quad (1)$$

Here  $f(\mathbf{c}_n)$  corresponds to the fluorescence signal from the experimental well of  $\mathbf{c}_n$ , while  $\bar{f}_{blank}$  and  $\bar{f}_{control}$  denote the median fluorescence signal from the blank and untreated wells, respectively. Notably, the variable  $\mathbf{c}_n$  is a vector that contains the individual concentrations of all  $d$  compounds of the  $n$ th cocktail studied, denoted  $c_{1n}, c_{2n}, \dots, c_{dn}$ . For drugs causing growth inhibition and/or cell killing the range of  $S$  spans from 0 to 1 indicating minimal and maximal cell survival respectively, compared to untreated cells. All generated data can be found at [27–30].

### Label-free live-cell imaging

Phase-contrast time-lapse images were acquired using the IncuCyte S3 (Sartorius) located inside the incubator. The microscope had a 10× objective with the ability to capture high quality phase-contrast microscopy images, 800 × 992 pixels each. 18 frames/images per experimental well were acquired, one every 4h for 68h starting without treatment at 0h. All generated data can be found at [27–30].

### Programming environment and computing resources

COMBImageDL was developed in MATLAB R2019b (The MathWorks, Inc., Natick, Massachusetts, United States). It is distributed as a MATLAB application, as well as a standalone desktop application for non-MATLAB Windows users [31]. All data analyses in the context of this work were performed in a single computer with an Intel Core i7-6700HQ CPU, quad-core 2.6 Hz, 32 GB RAM, GeForce GTX 970M GPU, MATLAB R2022b and CUDA Toolkit 11.2.

## 3. Results

### 3.1. COMBImageDL

The design and analyses of the exhaustive CUSP9 *in vitro* experiment were performed by means of COMBImageDL [31,32], a DL improved version of our recently reported framework, COMBImage2 [20]. It consists of 6 different modules (COMBO-Pick, COMBO-C, COMBO-M, COMBO-MF, COMBO-V and COMBO-Mine), which were employed to design the required 384-well plate layouts (COMBO-Pick), extract 4 different types of drug induced response patterns (described below) and perform data fusion and mining (COMBO-Mine) to discover prototypical response behaviors and discern higher- from lower- and single-drug effects. The 4 different types of extracted response patterns include endpoint quantification of cell viability (COMBO-V) and temporal quantification of cell growth/confluence (COMBO-C), changes in cell morphology (COMBO-M) and apoptotic-like cell counts (COMBO-MF). The methodology and functionality of the 6 aforementioned modules are thoroughly described in our earlier work [20]. Here, we improved foreground/background segmentation by replacing our previous segmentation algorithm [20] with a slightly modified, less complex version of U-Net [32–34]; a deep convolutional neural network for semantic segmentation.

**Table 1**

**CUSP9v3 drugs and concentrations.** Fixed concentrations selected and used for the exhaustive *in vitro* experiment.

Drug	Concentration (μM)	Abbreviation
aprepitant	3	Apr
auranofin	0.15	Aur
captopril	2	Cap
celecoxib	2	Cel
disulfiram	1.4	Dis
itraconazole	2	Itr
minocycline	6	Min
sertraline	0.9	Ser
ritonavir	12	Rit
temozolomide	30	TMZ

#### 3.1.1. Automated experimental design

The experimental module COMBO-Pick was employed to generate the plate layouts for the exhaustive CUSP9 *in vitro* experiment. COMBO-Pick distributed the exhaustive experiment across two 384-well plates; one with all single drugs and drug cocktails up to order 4 (260 treated and 48 untreated wells) and a second one with all drug cocktails from order 5 to 9 (261 treated and 47 untreated wells). Each plate was replicated 4 times. The 8 generated plate layouts were used together with an in-house software, Bridge [17], to produce the corresponding transfer schemes needed for acoustic liquid dispensation performed by an Echo 550 (Labcyte Inc., Sunnyvale, CA).

#### 3.1.2. Extraction of drug induced response patterns

The computational modules COMBO-V, COMBO-C, COMBO-M and COMBO-MF were employed to perform endpoint cell viability analyses (Fig. 1) and temporal quantification of cell culture confluence/growth, changes in cell culture morphology and apoptotic-like cell counts, respectively. Integrated intra- and inter-plate quality control (QC) procedures were employed in order to eliminate outliers that may cause large variability in the image quality between different time points, experimental wells and replicate plates.

More specifically, following the automated QC routines introduced in our previous work [20], the 4 inter-plate replicate results were merged by calculating the median, in order to reduce experimental variability. To quantify uncertainty and detect deviations from untreated control wells, the inter-plate results were calculated and visualized based on the following resampling based approach.

One untreated well was randomly selected with replacement from each of the 4 replicate plates and the median value for the corresponding extracted features was calculated. This sampling procedure was repeated  $N = 10^6$  times and resulted in a null distribution of median values (i.e., how large values after calculating the median could be expected by random chance in untreated wells) assuming only one untreated experimental well per plate, exactly as for the treated wells. Finally, the 10th, 50th, 90th percentiles of the null distribution per time point were plotted together with the corresponding values for the treated wells. Statistically significant drug induced effects were indicated only when lying below the 10th or above the 90th percentile of the null distribution, respectively (Figs. 1–2).

Fig. 2 shows temporal changes in cell culture morphology for all drug combinations up to order four for the patient derived GBM cell line U3082, after quality control of the four replicate experimental plates. Reading, comparing and evaluating temporal responses of large-scale drug combination experiments is indeed challenging. The purpose of Fig. 2 is not to enable the reader to read off individual temporal responses (although it is possible when zooming in with any standard PDF viewer), but rather stressing the importance of using clustering methods to analyze and visualize the results, which is further described in the following section.

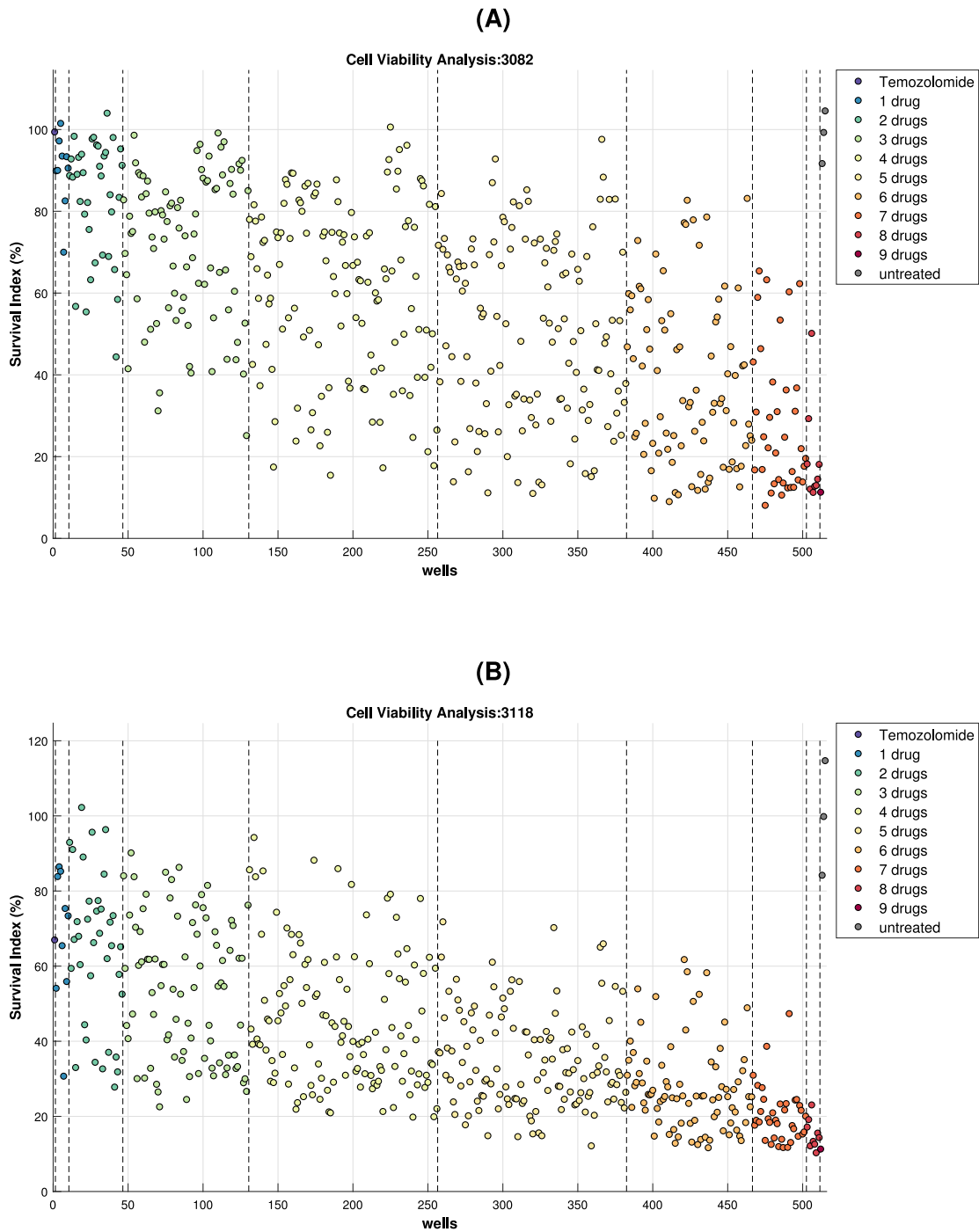


**Fig. 1.** Cell viability results for the GBM cell lines (A) U3082 and (B) U3118 covering all CUSP9 subsets (combined with TMZ) after QC. Each data point corresponds to a particular drug treated well starting from TMZ alone and going up until all CUSP9 drugs are combined with TMZ. The median survival index (%) across the 4 replicate plates is shown. The 3 gray data points at the end correspond to the 10th, 50th, 90th percentiles of the null distribution of untreated wells. Deviations from the 10th and 90th percentiles suggest statistically significant effects. The vertical dotted lines are used to mark the borders between the different drug combination orders that might be difficult to discern otherwise.

The temporal changes in cell culture morphology illustrated in Fig. 2 are quantified by means of the COMBO-M module of COMBImageDL as:

$$\Delta M_w(t_i) = \frac{\|\mathbf{h}_w(t_i) - \mathbf{h}_w(t_0)\|_1}{\|\mathbf{h}_w(t_0)\|_1}, \quad t_0 \leq t_i \leq t_{n-1} \quad (2)$$

where  $\mathbf{h}_w(t_i)$  is the feature vector describing the morphology of time point  $t_i$  of an experimental well  $w$ . Therefore,  $\Delta M_w$  is a relative measure of change in cell culture morphology, which gives the value zero at the first time point  $t_0$  and subsequently positive values at later time points if

the morphological changes are increasing. This relative measure establishes a reference value  $\Delta M_w(t_0) = 0$  and compensates for differences in cell seeding that otherwise makes the results difficult to compare between different experimental wells. By employing Eq. (2) for all available time points in the interval  $[t_0, t_{n-1}]$ , a temporal curve showing changes in cell culture morphology is obtained for every experimental well  $w$ . Such a temporal curve together with the corresponding percentile curves determined from the untreated control wells are shown in each and every subplot of Fig. 2.

## Change in Morphology (%) : 3082



**Fig. 2.** Temporal changes in cell morphology for the GBM cell line U3082. All CUSP9 subsets (combined with TMZ) from order 1 to 4 after QC are shown as an example. For a particular CUSP9 subset, the median curve across the 4 replicate plates (solid colored trace) is jointly shown with the corresponding median (solid black trace) curve of TMZ alone and the 10th, 50th, 90th percentiles of the null distribution of untreated wells (striped black traces). Deviations from the 10th and 90th percentiles suggest statistically significant effects. Time in hours (starting at 0h without treatment) is shown in the x-axis, while the change in cell morphology (%) with respect to 0h is shown in the y-axis. The first two letters of the individual drugs combined with TMZ are shown on the title of each subplot.

### 3.1.3. Temporal data fusion and mining

The computational module COMBO-Mine was used to merge all 4 types of extracted response patterns and perform temporal data mining. The overarching goal was to explore the large combinatorial response space in a data-driven way by organizing the observed drug combination effects into groups with distinct prototypical response behaviors. This organization is based on top-down hierarchical clustering, using the K-means algorithm, with  $K = 2$  at each level, as thoroughly described in our earlier work [20,32]. The aim here was to acquire a hierarchy of prototypical response patterns and associate them with the unique single drugs and/or drug cocktails causing them. Using this methodology, we were able to discriminate higher- from lower- and single-drug effects without any specific assumption about the drug interactions [32]. Notably, all drugs/drug combinations that belong to such a unique subset are ranked equally much, as they are part of the same group.

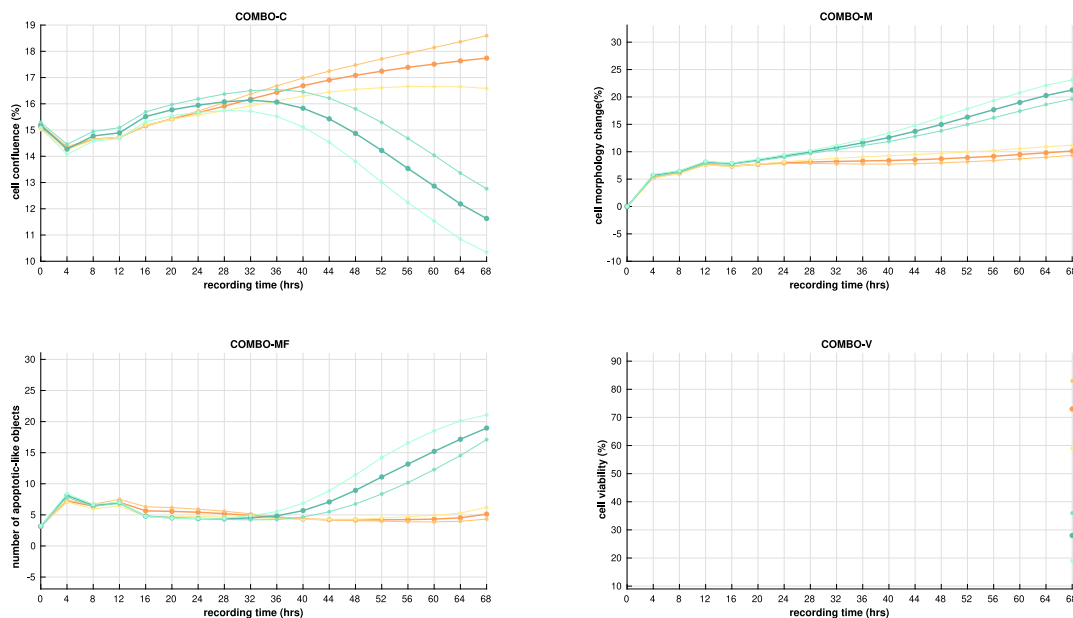
The employment of COMBO-Mine for the exhaustive *in vitro* evaluation of the CUSP9v3 protocol revealed 2 main groups of response patterns with 2 subgroups each (Fig. 3). Each (sub)group is visualized by the corresponding four average response patterns; temporal changes in cell culture confluence and morphology quantified by COMBO-C and COMBO-M respectively, temporal induction of apoptotic-like cell counts (of particular size) quantified by COMBO-MF and endpoint cell viability determined by COMBO-V. In both cases, a distinct group of interesting behavioral patterns was observed, including increased cell culture growth inhibition, changes in cell morphology compared to untreated cells, increased apoptotic-like cell counts and decreased cell viability compared to untreated cells. The dynamics and amplitude of the drug induced responses differ between the two GBM stem-like cell lines indicating a heterogeneous response pattern, which has already been reported by previous studies [15] and could be easily attributed

to the inter-tumor heterogeneity of GBM, which might necessitate personalized adjustment of the CUSP9v3 protocol.

As mentioned earlier, each and every group of prototypical response patterns is characterized by the smallest set of single drugs and drug combinations in it (Fig. 4) in order to discern higher- from lower-order and single-drug effects. This type of analysis revealed that the distinct group of interesting response patterns described above were consisting only of 3–6 drugs (as add-on to TMZ). Notably, the observed response was equivalent or even higher in some cases than the whole 9-drug combination. Although most of the unique potent lower-order drug combinations differ among the two GBM cell lines employed (Fig. 4), the four-order drug combination Aur, Dis, It and Ser appears to be their common denominator. The correspondingly induced responses were associated with reduced cell growth, increased changes in cell culture morphology and increased number of apoptotic-like cell counts already at 4–28 hours of treatment, as well as highly reduced cell viability compared to untreated cells at 68 hours of treatment (Figs. 5–6).

Notably, Figs. 3 and 4 are related but different. Fig. 3 illustrates the centroids obtained from employing K-means clustering (with  $K=2$ ) at two hierarchical levels, resulting in six color lines, three colors per cluster. Looking at the first hierarchical level, two clusters are observed related to two prototypical behaviors, shown in dark orange and dark green accordingly. These two first level clusters are named as “Level 1 - Orange Cluster” and “Level 1 - Green Cluster” in Fig. 4. At the second hierarchical level, K-means (with  $K = 2$ ) is employed using the clusters/groups from the first level and the corresponding centroids are visualized in a similar way using different nuances of orange and green colors to indicate their origin. Fig. 4 shows the results of the exhaustive subset search employed at both hierarchical clustering levels. In other words, every group/cluster is characterized by the smallest set of single drugs and drug combinations in it.

(A) U3082



(B) U3118

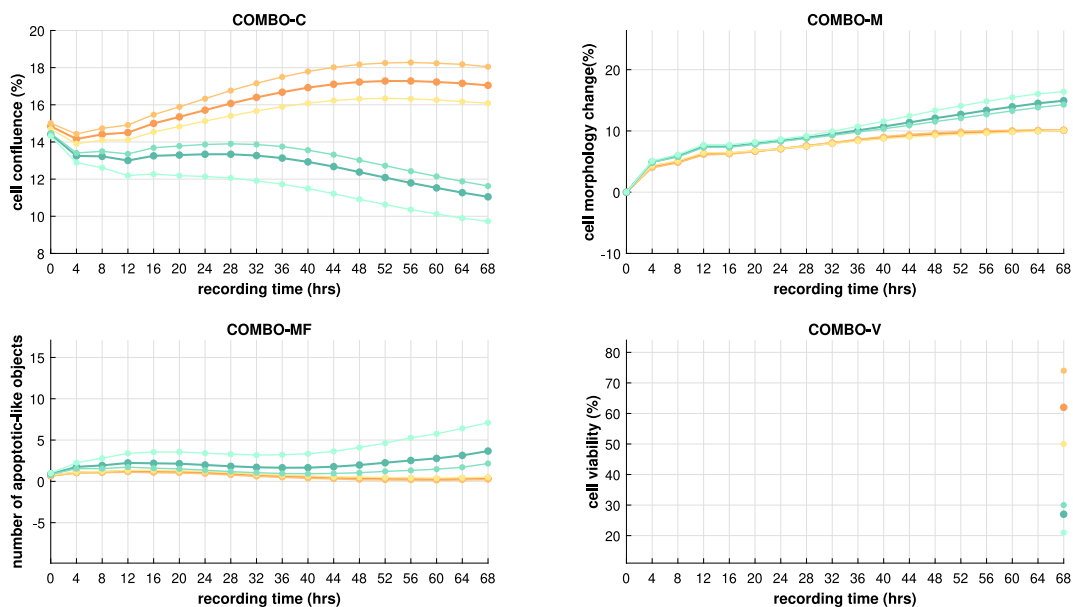


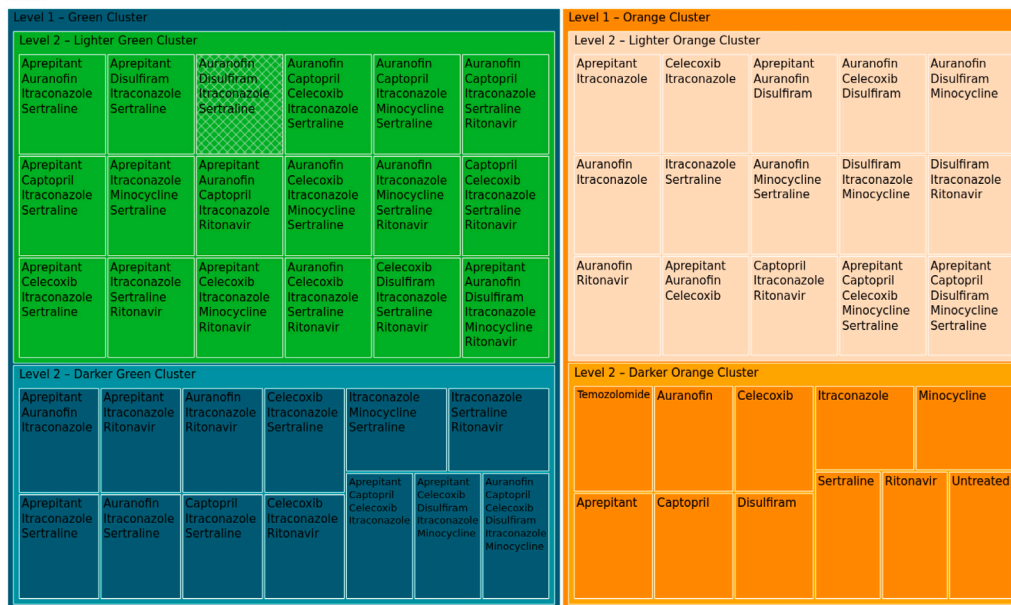
Fig. 3. Temporal data mining for the GBM cell lines (A) U3082 and (B) U3118. The employment of COMBO-Mine for the exhaustive *in vitro* evaluation of the CUSP9 protocol revealed 2 main groups with 2 subgroups each. Each (sub)group is visualized by the corresponding four average response patterns (three live-cell imaging based profiles and one endpoint cell viability value) and annotated only by the unique set of drugs and/or drug cocktails included in it. Groups of single drugs and drug combinations demonstrating enhanced *in vitro* efficacy are represented in green.

To exemplify, let us assume that there are two drugs  $x$  and  $y$  at concentrations  $c_x$  and  $c_y$ , respectively. If the two multi dimensional response patterns  $f(c_x)$  and  $f(c_x, c_y)$  form together a particular group/cluster  $A$  with an average prototypical response profile denoted  $\bar{f}_A$ , then the exhaustive subset search identifies  $c_x$  as representative of  $\bar{f}_A$ . In this context, Fig. 3 shows the average prototypical response profile  $\bar{f}_A$ , whereas Fig. 4 shows the name of the representative drug  $x$  (equivalent to  $c_x$  since there is only one fixed concentration). The color convention between Figs. 3 and 4 is kept the same to facilitate interpretations. In particular, single drugs and drug combinations belonging to a higher and lower level are visualized using the color of the higher/top

level in order to be able to trace their origin when interpreting the corresponding results.

For example, if we look at the bottom chart of Fig. 4 and focus on the left upper part that corresponds to the results for the green cluster, we can see that in “Level 2 - Darker Green Cluster”, there is only one drug combination, namely (Aur, Dis, Ser, Rit) that actually has the color of level 2. All the rest are shown in even darker green, which is the color of level 1. This means that all these combinations originate from the cluster of the first level and they are not unique to the second level. This shows that the only unique combination in this case is (Aur, Dis, Ser, Rit), which has the color of the second level. Taken together, this means that this new combination and the others identified already at level 1,

U3082



U3118

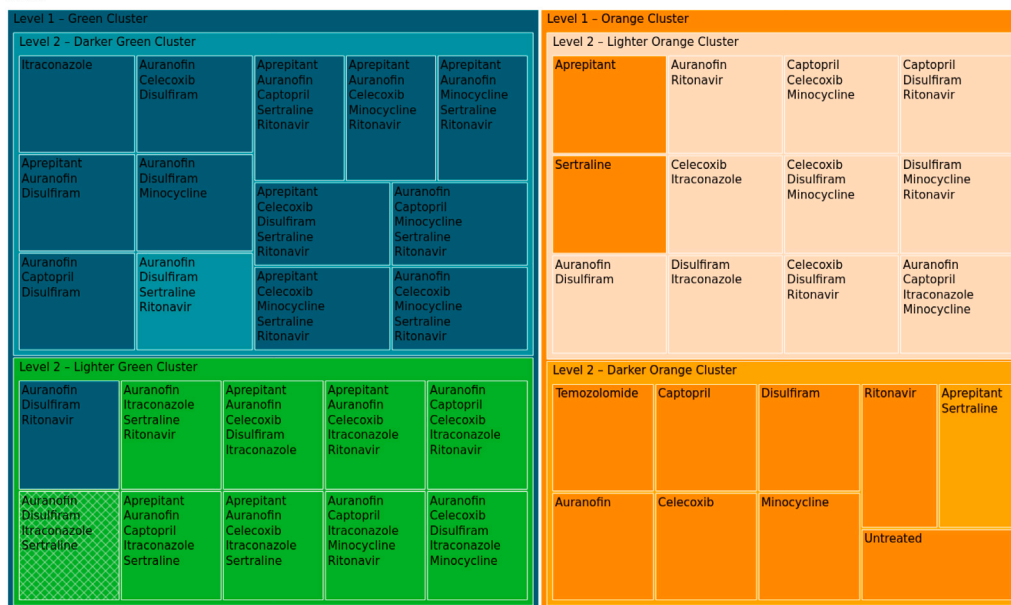


Fig. 4. Exhaustive subset search of all 511 CUSP9v3 subsets for the GBM cell lines U3082 (top) and U3118 (bottom). The colors used match the colors used in Fig. 3 to facilitate understanding. Every hierarchical level has a distinct color. However, single drugs and drug combinations belonging to a higher and lower level are visualized using the color of the top level in the hierarchy to trace their origin when interpreting the corresponding results. Single drugs and drug combinations demonstrating enhanced *in vitro* efficacy are represented in green.

all induce approximately the same four response patterns (confluence, morphology, apoptosis-like, cell viability). In Fig. 3 these patterns are represented by the four level-2 cluster prototypes that have the darker green color among the prototypes corresponding to level 2.

#### 4. Discussion

This study reports the first exhaustive *in vitro* evaluation of the CUSP9v3 protocol [4–8], which has already completed a phase Ib/IIa clinical trial (NCT02770378) as add-on treatment to standard-of-care temozolomide (TMZ), exhibiting a favorable safety profile for the nine evaluable patients included [8].

Here, all 511 plausible subsets were studied for the first time *in vitro* using quantitative label-free live-cell imaging jointly coupled with single endpoint cell viability analyses. Thanks to our automated and standardized plate design module, we were able to replicate the whole experiment 4 independent times through a layout of eight 384-well plates rapidly, efficiently and without involving any manual step. These independent inter-plate measurements allowed us to benefit not only from (non-parametric) resampling based QC, but also to quantify uncertainty in the obtained results by taking into account the associated technical and biological variability. This built-in quantification of uncertainty is very valuable as it helps avoiding potential misinterpretations due to technical and biological variability.

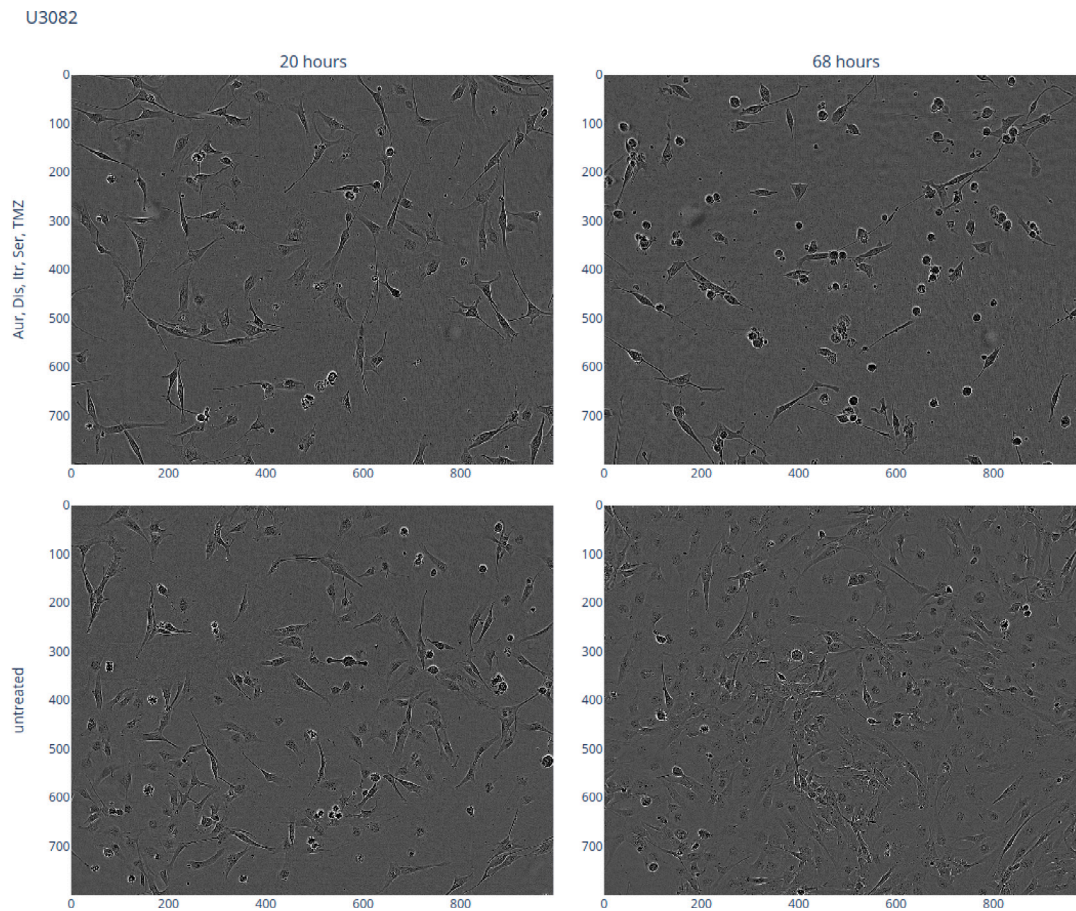


Fig. 5. Morphological changes over time for the GBM cell line U3082. Two time points (20 and 68 hours) of the recorded *in vitro* growing cell populations are shown under treatment with Aur, Dis, Itr and Ser as add-on to TMZ (upper row), as well as when no treatment is added (lower row).

To discern higher- from lower- and single-drug effects among all 511 tested subsets, we employed our tailor made and previously introduced data driven methodology [20,32]. We identified hierarchies of prototypical response patterns (in terms of cell culture growth, changes in cell culture morphology, apoptotic-like cell counts and cell viability), as well as all single drugs and/or drug combinations primarily associated with these prototypical behaviors (Fig. 3). This analysis revealed several lower-order CUSP9v3 subsets that had an equivalent or even higher *in vitro* effect than the whole 9-drug cocktail when used as add-on to TMZ (Fig. 4). The finding above is interesting as it demonstrates that the CUSP9 regimen could be potentially replaced by smaller drug subsets, especially after being further studied *in vivo*. Moreover, the majority of lower-order drug combinations found to induce enhanced *in vitro* effects were different for the two GBM stem-like cell lines employed (Fig. 4), indicating the importance for setting up systematic procedures to guide personalized combination therapy selection in the clinic.

These conclusions would have been impossible without an exhaustive *in vitro* evaluation, like the one performed here. Although we have only used two proneural GBM cell lines from the HGCC resource [21], our findings illustrate the feasibility and importance of such comprehensive evaluations of higher-order drug cocktails, including and beyond CUSP9. In complex and heterogeneous diseases, like GBM, personalized rather than one-size-fits-all pharmacotherapies seems to be the only successful way forward, especially when they consist of multiple drugs [35]. In this sense, the CUSP9 cocktail constitutes a very promising therapeutic route but its potential to be further optimized at an individualized level has not been investigated yet. Notably, the purpose of this study was not restricted solely to identify CUSP9 subsets with retained anti-tumoral potency, but rather demonstrate the general

feasibility of performing, analyzing and interpreting exhaustive *in vitro* experiments by means of COMBImageDL.

Notably, a specific five-drug combination, comprising Aur, Dis, Itr, Ser, and TMZ, has demonstrated increased anti-tumoral efficacy across both utilized patient-derived GBM cell lines (Fig. 4). While the validation of this finding across a broader spectrum of GBM tumors and more complex models is imperative, it is equally crucial to explore the primary molecular pathways implicated in GBM and speculate on how they might be perturbed *in vitro* by the synergistic potential of these five drugs. Their combined impact on fundamental cellular processes such as survival, apoptosis, oxidative stress, and DNA damage appears pivotal. Specifically, Aur and Dis may intensify oxidative stress, potentially amplifying TMZ-induced DNA damage. Additionally, disruption of cell survival pathways, including the NF- $\kappa$ B pathway, known to be modulated by both Aur and Dis, could diminish survival signals in GBM cells, potentially enhancing the effects of TMZ. Dis-induced proteasome inhibition might disturb protein homeostasis, rendering GBM cells more susceptible to other treatments. Itr-induced Hedgehog pathway inhibition could influence GBM cell proliferation and stem cell-like properties. Although the *in vitro* effect of Ser, a serotonin uptake inhibitor, is more challenging to explain, it could be attributed to off-target effects, potentially involving the modulation of cellular stress responses or interactions with other neurotransmitter-related pathways.

The growing demand and increasing interest in higher-order drug regimens in clinical oncology, exemplified by regimens like CUSP9 [4–8], MEMMAT [36], and ABC7 [37], underscore the current momentum in molecular and systems biomedicine. The combination of a robust theoretical foundation and an advanced experimental–computational framework, as presented in this study, holds great potential for further

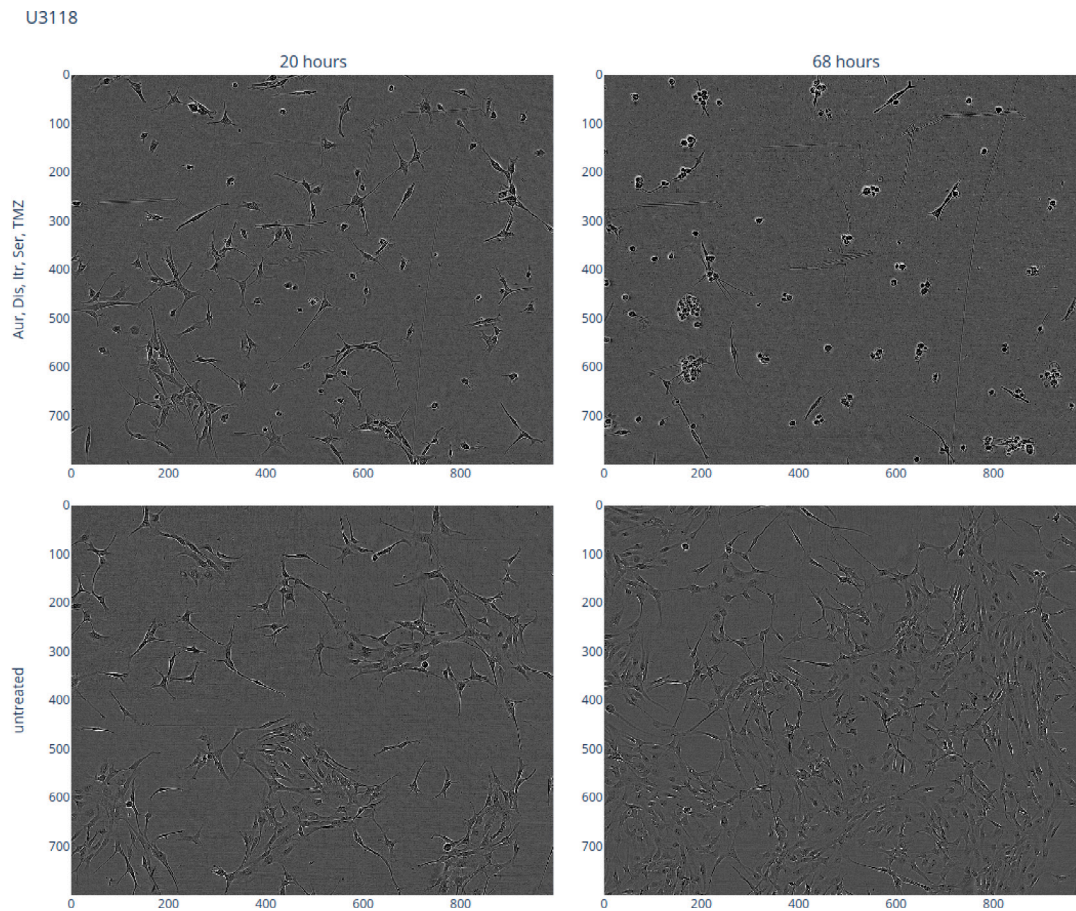


**Fig. 6.** Morphological changes over time for the GBM cell line U3118. Two time points (20 and 68 hours) of the recorded *in vitro* growing cell populations are shown under treatment with Aur, Dis, Itr and Ser as add-on to TMZ (upper row), as well as when no treatment is added (lower row).

integration into clinical pharmacology practices. We anticipate that COMBImageDL will serve as a valuable tool, complementing traditional approaches that rely on cytotoxic endpoints and single drug sensitivity testing [17,18], by incorporating quantitative live-cell imaging and the assessment of higher-order drug combinations.

## 5. Limitations

Further investigation along this trajectory is essential to determine the extent to which the observed drug combination response patterns in this study are applicable to a wider spectrum of GBM tumors. Additionally, it is crucial to understand how these findings translate into more complex *in vivo* studies downstream. We acknowledge the existence of more intricate aspects that require exploration. The effects of drugs need to be studied within the tumor microenvironment, encompassing elements such as angiogenesis, stromal interactions, immune cell infiltration, and the role of drug metabolites exclusive to *in vivo* conditions. Despite these complexities, we emphasize the pivotal role of a comprehensive *in vitro* evaluation as an indispensable precursor, a step that should consistently be undertaken in the early stages of pre-clinical assessments, even within repurposing strategies.

## 6. Conclusions

A subset of four CUSP9 drugs (auranofin, disulfiram, itraconazole, sertraline) was found to be potent in both *in vitro* models studied, showing reduced cell growth, notable changes in cell culture morphology, an increased number of apoptotic-like cell counts as early as 4-28 h into treatment, and significantly decreased cell viability compared to untreated cells after 68 h.

As a specific practical recommendation, we suggest that *in vitro* sensitivity testing of GBM patient cells should encompass the entire CUSP9 cocktail, along with some of the identified lower-order subsets that adhere to clinical standards and pharmacological practices. For instance, findings from a corresponding phase Ib/IIa clinical trial (NCT02770378) indicated that ritonavir, captopril, itraconazole and temozolomide were the drugs most frequently requiring dose modification or pausing due to adverse events. Therefore, a strategic approach would involve selecting drug combinations from the identified list that minimize the use of these four drugs for further exploration and testing in more complex systems. Notably, such an example is the five-drug combination discovered in this study and discussed in more detail above; comprising auranofin, disulfiram, itraconazole, sertraline and temozolomide. Such an experimental set up coupled with more complex models would offer initial insights into whether a patient should undergo treatment with all 9 drugs, particularly in situations where exhaustive evaluations may not be practical.

## Abbreviations

Apr: aprepitant; Aur: auranofin; Cap: captopril; Cel: celecoxib; Dis: disulfiram; GBM: glioblastoma; HGCC: Human Glioblastoma Cell Culture; Itr: itraconazole; Min: minocycline; QC: quality control; Rit: ritonavir; Ser: sertraline; TMZ: temozolomide

## CRediT authorship contribution statement

**Efthymia Chantzi:** Writing – review & editing, Writing – original draft, Visualization, Validation, Software, Methodology, Investigation, Formal analysis, Data curation, Conceptualization. **Ulf Hammerling:** Writing – review & editing, Supervision, Resources, Investigation.

**Mats G. Gustafsson:** Writing – review & editing, Supervision, Resources, Project administration, Methodology, Investigation, Funding acquisition, Conceptualization.

### Declaration of competing interest

The authors declare that they have no conflict of interest to disclose.

### Acknowledgments

We thank the RCL (Resistenstest cancerläkemedel) team at Uppsala University Hospital, division of Clinical Chemistry and Pharmacology, for the service project performed by them to generate the experimental data used and presented in this paper. We also thank the anonymous reviewers for their valuable feedback.

### Funding

This research work was supported by the Swedish Research Council (grant no. 2017-04655).

### References

- O.G. Taylor, J.S. Brzozowski, K.A. Skelding, Glioblastoma multiforme: An overview of emerging therapeutic targets, *Front. Oncol.* 9 (2019) 963.
- M.A. Qazi, P. Vora, C. Venugopal, S.S. Sidhu, J. Moffat, C. Swanton, S.K. Singh, Intratumoral heterogeneity: Pathways to treatment resistance and relapse in human glioblastoma, *Ann. Oncol.* 28 (7) (2017) 1448–1456.
- X. Lan, D.J. Jörg, F.M.G. Cavalli, L.M. Richards, L.V. Nguyen, R.J. Vanner, P. Guilhamon, L. Lee, M.M. Kushida, D. Pellacani, N.I. Park, F.J. Coutinho, H. Whetstone, H.J. Selvadurai, C. Che, B. Luu, A. Carles, M. Moxa, N. Rastegar, R. Head, S. Dolma, P. Prinos, M.D. Cusimano, S. Das, M. Bernstein, C.H. Arrowsmith, A.J. Mungall, R.A. Moore, Y. Ma, M. Gallo, M. Lupien, T.J. Pugh, M.D. Taylor, M. Hirst, C.J. Eaves, B.D. Simons, P. Dirks, Fate mapping of human glioblastoma reveals an invariant stem cell hierarchy, *Nature* 549 (7671) (2017) 227–232.
- M.E. Halatsch, A. Dwucet, C.J. Schmidt, J. Hlnickel, T. Heiland, K. Zeiler, M.D. Siegelin, R.E. Kast, G. Karpel-Massler, In vitro and clinical compassionate use experiences with the drug-repurposing approach CUSP9v3 in glioblastoma, *Pharmaceuticals (Basel)* 14 (12) (2021).
- R.E. Kast, J.A. Boockvar, A. Bruning, F. Cappello, W.W. Chang, B. Cvek, Q.P. Dou, A. Duenas-Gonzalez, T. Efferth, D. Focosi, S.H. Ghaffari, G. Karpel-Massler, K. Ketola, A. Khoshnevisan, D. Keizman, N. Magne, C. Marosi, K. McDonald, M. Munoz, A. Paranjpe, M.H. Pourgholami, I. Sardi, A. Sella, K.S. Srivenugopal, M. Tuccori, W. Wang, C.R. Wirtz, M.E. Halatsch, A conceptually new treatment approach for relapsed glioblastoma: coordinated undermining of survival paths with nine repurposed drugs (CUSP9) by the International Initiative for Accelerated Improvement of Glioblastoma Care, *Oncotarget* 4 (4) (2013) 502–530.
- R.E. Kast, G. Karpel-Massler, M.E. Halatsch, CUSP9\* treatment protocol for recurrent glioblastoma: Aprepitant, artesunate, auranofin, captopril, celecoxib, disulfiram, itraconazole, ritonavir, sertraline augmenting continuous low dose temozolomide, *Oncotarget* 5 (18) (2014) 8052–8082.
- Marc-Eric Halatsch, Michael Salacz, Bernd Schmitz, Georg Karpel-Massler, Richard Kast, EXTH-79. Initial experiences with compassionate-Use CUSP9v3/v4 for recurrent glioblastoma, *Neuro-Oncol.* 19 (Suppl 6) (2017) vi90.
- M.E. Halatsch, R.E. Kast, G. Karpel-Massler, B. Mayer, O. Zolk, B. Schmitz, A. Scheuerle, L. Maier, L. Bullinger, R. Mayer-Steinacker, C. Schmidt, K. Zeiler, Z. Elshaer, P. Panther, B. Schmelzle, A. Hallmen, A. Dwucet, M.D. Siegelin, M.A. Westhoff, K. Beckers, G. Bouche, T. Heiland, A phase Ib/IIa trial of 9 repurposed drugs combined with temozolomide for the treatment of recurrent glioblastoma: CUSP9v3, *Neurooncol. Adv.* 3 (1) (2021).
- Haojie Jin, Liqin Wang, René Bernards, Rational combinations of targeted cancer therapies: background, advances and challenges, *Nat. Rev. Drug Discov.* 22 (3) (2023) 213–234.
- Timothy Johanssen, Laura McVeigh, Sara Erridge, Geoffrey Higgins, Joelle Straehla, Margaret Frame, Tero Aittokallio, Neil O. Carragher, Daniel Ebner, Glioblastoma and the search for non-hypothesis driven combination therapeutics in academia, *Front. Oncol.* 12 (2023) 1075559.
- Naiara Perurena, Lisa Situ, Karen Cichowski, Combinatorial strategies to target RAS-driven cancers, *Nat. Rev. Cancer* (2024) 1–22.
- Freya R. Weth, Georgia B. Hoggarth, Anya F. Weth, Erin Paterson, Madeleine P.J. White, Swee T. Tan, Lifeng Peng, Clint Gray, Unlocking hidden potential: Advancements, approaches, and obstacles in repurposing drugs for cancer therapy, *Br. J. Cancer* 130 (5) (2024) 703–715.
- Qiyu Cao, Annika Hajosch, Richard Eric Kast, Christopher Loehmann, Michal Hlavac, Pamela Fischer-Posovszky, Hannah Strobel, Mike-Andrew Westhoff, Markus D. Siegelin, Christian Rainer Wirtz, et al., Tumor treating fields (TTFields) combined with the drug repurposing approach CUSP9v3 induce metabolic reprogramming and synergistic anti-glioblastoma activity in vitro, *Br. J. Cancer* (2024) 1–12.
- Angharad N. de Cates, Matthew R.B. Farr, Nicola Wright, Morag C. Jarvis, Karen Rees, Shah Ebrahim, Mark D. Huffman, Fixed-dose combination therapy for the prevention of cardiovascular disease, *Cochrane Database Syst. Rev.* (4) (2014).
- E. Skaga, I.Ø. Skaga, Z. Grieg, C.J. Sandberg, I.A. Langmoen, E.O. Vik-Mo, The efficacy of a coordinated pharmacological blockade in glioblastoma stem cells with nine repurposed drugs using the CUSP9 strategy, *J. Cancer Res. Clin. Oncol.* 145 (6) (2019) 1495–1507.
- J.L. Wilding, W.F. Bodmer, Cancer cell lines for drug discovery and development, *Cancer Res.* 74 (9) (2014) 2377–2384.
- K. Blom, P. Nygren, J. Alvarsson, R. Larsson, C.R. Andersson, Ex vivo assessment of drug activity in patient tumor cells as a basis for tailored cancer therapy, *J. Lab. Autom.* 21 (1) (2016) 178–187.
- K. Blom, P. Nygren, R. Larsson, C.R. Andersson, Predictive value of ex vivo chemosensitivity assays for individualized cancer chemotherapy: A meta-analysis, *SLAS Technol.* 22 (3) (2017) 306–314.
- Yann LeCun, Yoshua Bengio, Geoffrey Hinton, Deep learning, *Nature* 521 (7553) (2015) 436.
- E. Chantzi, M. Jarvius, M. Niklasson, A. Segerman, M.G. Gustafsson, COMBImage2: A parallel computational framework for higher-order drug combination analysis that includes automated plate design, matched filter based object counting and temporal data mining, *BMC Bioinform.* 20 (1) (2019) 304.
- Y. Xie, T. m, Y. Jiang, P. Johansson, V.D. Marinescu, N. Lindberg, A. Segerman, G. Wicher, M. Niklasson, S. Baskaran, S. Sreedharan, I. Everlien, M. Kastemar, A. Hermansson, L. Elfineh, S. Libard, E.C. Holland, G. Hesselager, I. Alafuzoff, B. Westermarck, S. Nelander, K. Forsberg-Nilsson, L. Uhrbom, The human glioblastoma cell culture resource: Validated cell models representing all molecular subtypes, *EBioMedicine* 2 (10) (2015) 1351–1363.
- European medicines agency, 2023, <https://www.ema.europa.eu/en/medicines>. (Online; Accessed 16 November 2023).
- Electronic medicines compendium, 2023, <https://www.medicines.org.uk/emc>. (Online; Accessed 16 November 2023).
- C. Roder, M.J. Thomson, Auranofin: Repurposing an old drug for a golden new age, *Drugs R D* 15 (1) (2015) 13–20.
- M. Schulz, S. Iwersen-Bergmann, H. Andresen, A. Schmoltdt, Therapeutic and toxic blood concentrations of nearly 1,000 drugs and other xenobiotics, *Crit. Care* 16 (4) (2012) R136.
- E. Lindhagen, P. Nygren, R. Larsson, The fluorometric microculture cytotoxicity assay, *Nat. Protoc.* 3 (8) (2008) 1364–1369.
- Chantzi, Efthymia (2023) “CUSP9v3-U3082-part1”, Mendeley data, V1, 2023, <http://dx.doi.org/10.17632/fkx3s4vxfn.1>, (Online; Accessed 16 November 2023).
- Chantzi, Efthymia (2023) “CUSP9v3-U3082-part2”, Mendeley data, V1, 2023, <http://dx.doi.org/10.17632/gd69567gh2.1>, (Online; Accessed 16 November 2023).
- Chantzi, Efthymia (2023) “CUSP9v3-U3118-part1”, Mendeley data, V1, 2023, <http://dx.doi.org/10.17632/g92xx8wcvp.1>, (Online; Accessed 16 November 2023).
- Chantzi, Efthymia (2023) “CUSP9v3-U3118-part2”, Mendeley data, V1, 2023, <http://dx.doi.org/10.17632/5jk89vphb2.1>, (Online; Accessed 16 November 2023).
- COMBImageDL, 2023, <https://github.com/EffieChantzi/COMBImageDL.git>. (Online; Accessed 16 November 2023).
- Efthymia Chantzi, Algorithmic Discovery, Development and Personalized Selection of Higher-Order Drug Cocktails (Ph.D. thesis), Uppsala University, 2020.
- Olaf Ronneberger, Philipp Fischer, Thomas Brox, U-net: Convolutional networks for biomedical image segmentation, in: Nassir Navab, Joachim Hornegger, William M. Wells, Alejandro F. Frangi (Eds.), *Medical Image Computing and Computer-Assisted Intervention – MICCAI 2015*, Springer International Publishing, Cham, 2015, pp. 234–241.
- T. Falk, D. Mai, R. Bensch, Ö. Çiçek, A. Abdulkadir, Y. Marrakchi, A. Böhm, J. Deubner, Z. Jäckel, K. Seiwald, A. Dovzhenko, O. Tietz, C. Dal Bosco, S. Walsh, D. Saltukoglu, T.L. Tay, M. Prinz, K. Palme, M. Simons, I. Diester, T. Brox, O. Ronneberger, Author Correction: U-Net: Deep learning for cell counting, detection, and morphometry, *Nat. Methods* 16 (4) (2019) 351.
- M.B. Serafin, A. Bottega, T.F. da Rosa, C.S. Machado, V.S. Foletto, S.S. Coelho, A.D. da Mota, R. rner, Drug repositioning in oncology, *Am. J. Ther.* 28 (1) (2021) e111–e117.
- Andreas Peyrl, Monika Chocholous, Amedeo Azizi, Mark Kieran, Karsten Nysom, Jaroslav Sterba, Magnus Sabel, Thomas Czech, Karin Dieckmann, Christine Haberler, Maresa Schmoock, Ulrike Leiss, Irene Slavc, MB-70 MEMMAT - A phase II study of metronomic and targeted anti-angiogenesis therapy for children with recurrent/progressive medulloblastoma, *Neuro-Oncology* 18 (Suppl 3) (2016) iii113.
- R.E. Kast, N. Skuli, S. Cos, G. Karpel-Massler, Y. Shiozawa, R. Goshen, M.E. Halatsch, The ABC7 regimen: A new approach to metastatic breast cancer using seven common drugs to inhibit epithelial-to-mesenchymal transition and augment capecitabine efficacy, *Breast Cancer (Dove Med Press)* 9 (2017) 495–514.